

Clarifying the role of silver deposits on titania for the photocatalytic mineralisation of organic compounds

Hoang Tran, Jason Scott, Ken Chiang, Rose Amal*

ARC Centre for Functional Nanomaterials, School of Chemical Engineering and Industrial Chemistry,
The University of New South Wales, Sydney, NSW 2052, Australia

Received 11 August 2005; received in revised form 12 February 2006; accepted 13 February 2006
Available online 6 March 2006

Abstract

The effect of silver deposits on titanium dioxide on the photocatalytic mineralisation of various organic compounds was investigated. A series of fourteen organic compounds comprising C, H and O atoms alone, were assessed to gain insights into the influence of photodeposited silver. Photodeposition of the silver provided a bimodal distribution of silver deposit sizes, comprising of deposits less than 5 nm and deposits approximately 100 nm in diameter.

Silver deposits were found to promote, mildly deter or have a negligible effect on the mineralisation of the organics considered. Carboxylic acids generally experienced positive effects, deriving from their adsorption on TiO₂ and susceptibility to photogenerated hole attack. Increasing chain length and the presence of additional methyl groups decreased the positive effects. Alcohols did not benefit by the presence of silver due to their limited adsorption on TiO₂ at room temperature. Saccharides, while limited in their adsorption on TiO₂, experienced increases in mineralisation rates up to eight times following silver deposition. Carboxylic acids are generated as intermediates during the oxidation of saccharides whose degradation may be enhanced by the silver deposits rather than the saccharides directly. Aromatics did not encounter any positive effects due to silver deposits. The negligible effects are thought to derive from intermediates generated during the early stages of degradation facilitating charge recombination or limiting the access of other intermediates more susceptible to hole attack to the TiO₂ surface.

© 2006 Elsevier B.V. All rights reserved.

Keywords: Photocatalytic oxidation; Titanium dioxide; Silver; Mineralisation

1. Introduction

The deposition of metals such as Ag, Pt, Pd and Au on the surface of TiO₂ has been widely used to improve the photocatalytic activity of TiO₂ [1]. Silver is particularly suitable for industrial applications due to its low cost and simple preparation requirements [2,3]. Its effects have been studied for the degradation of various organics, as described in Table 1 for compounds containing C, H and O only and those containing N, S and Cl as well.

Table 1 indicates, in most instances, the presence of silver has a positive effect on the degradation of the organic compound in question. This enhanced photoactivity has been credited as predominantly a function of silver deposits behaving as electron traps during illumination, facilitating the sep-

aration of reduction and oxidation surface sites and lowering the extent of surface recombination [4,5]. The presence of Ag deposits can also improve the photoactivity by increasing TiO₂ surface area, depending on the method of preparation [6] although Arabatzis et al. [7] suggests other aspects such as surface features and surface chemistry cannot be disregarded. Surface area rarely increases during metal photodeposition, indicating any improvements are not due to surface area effects [3].

Table 1 also indicates the silver deposits are deleterious for degrading some organics. Reasons for the detrimental effects of silver deposits on photoactivity have been proposed including: (1) reduced access of the light to the TiO₂ surface due to excessive surface coverage by the silver deposits, especially at high silver loadings [8]; (2) blockage of the TiO₂ active sites by the metal deposits which are necessary for the photocatalytic process [9]; (3) an increase in charge carrier recombination rates at silver loadings above the optimum value, [10]; and (4) inhibition of the role of oxygen (as O₂⁻) in the photocatalytic process

* Corresponding author. Tel.: +61 2 9385 4361; fax: +61 2 9385 5966.
E-mail address: r.amal@unsw.edu.au (R. Amal).

Table 1
Effect of Ag deposits on the degradation of various organics

Organic	Formula	C–H bonds	C–O + C=O bonds	Ratio	Enhancement factor	TiO ₂ source	Ag deposition method	Ag/TiO ₂ loading	Ag deposit size (nm)	Reference
Containing C, H, O only										
Oxalic acid	C ₂ H ₂ O ₄	0	4	4	5	Degussa P25	Photodeposition	2.16 wt.%	n.r.r.	[19]
Acetone (gas)	C ₃ H ₆ O	6	1	0.17	1.3	Degussa P25	Photodeposition	0.5 (M ratio)	2	[20]
2-Propanol	C ₃ H ₈ O	7	1	0.14	2	Rutile	Photodeposition	0.5 wt.%	3–8	[4]
					0.86	Anatase	Photodeposition	0.5 wt.%	3–8	[4]
					1.2	Degussa P25	Photodeposition	3 wt.%	2–8	[10]
					1.5	Anatase (BDH) ^a	Photodeposition	3.4 wt.%	≤50	[10]
					4.1	Thin film (dip coat)	UV irradiation	8 wt.%	~15	[6]
Maleic acid	C ₄ H ₆ O ₅	3	5	1.7	4.1	Thin film (spray coat P25)	Impreg./precip	2 at.%	n.r.r.	[21]
<i>n</i> -Butanol (gas)	C ₄ H ₁₀ O	9	1	0.11	Detrimental	Thin film (spray coat P25)	Photodeposition	0.5 wt.%	n.r.r.	[12]
Phenol	C ₆ H ₆ O	5	1	0.2	3.3	Aldrich (anatase)	Photodeposition	65 wt.%	n.r.r.	[22]
					4.5	Aldrich (anatase)	Photodeposition	65 wt.%	n.r.r.	[22]
					2.9	Anatase (YCC) ^b	Photodeposition	1.046 wt.%	n.r.r.	[23]
					Negligible	Degussa P25	Photodeposition	2 at.%	~5	[6]
Salicylic acid	C ₇ H ₆ O ₃	5	3	0.6	Negligible	Degussa P25	Photodeposition	2 at.%	~5	[6]
Sucrose	C ₁₂ H ₂₂ O ₁₁	14	14	1	4	Degussa P25	Photodeposition	2 at.%	~5	[6]
					2.5	Degussa P25	Photodeposition	20 at.%	~2, 125	[3]
Containing C, H, O, N, S, Cl										
Chloroform	CHCl ₃	1	0	0	1.25	Aldrich (anatase)	Depos./precip.	1 wt.%	n.r.r.	[24]
Urea	CH ₄ N ₂ O	0	1	1	5.2	Aldrich (anatase)	Depos./precip.	1 wt.%	n.r.r.	[24]
Methyl mercaptan (gas)	CH ₃ SH	3	0	0	14	TiO ₂ dip-coated filter	Photodeposition	unclear	1–10	[25]
Trichloroethylene	C ₃ HCl ₃	1	0	0	1.6	Aldrich (anatase)	Photodeposition	1 wt.%	n.r.r.	[26]
2-Chlorophenol	C ₆ H ₅ OCl	4	1	0.25	1.5	Degussa P25	Photodeposition	6.4 × 10 ⁻⁴ wt.%	n.r.r.	[27]
Aniline	C ₆ H ₇ N	5	0	0	2	Degussa P25	Photodeposition	0.2 wt.%	n.r.r.	[28]
Methyl orange	C ₁₄ H ₁₄ N ₃ NaO ₃ S	14	0	0	2.3	Anatase	Depos./precip.	2 wt.%	10–16	[29]
					1.8	Thin film (spin coat)	UV irradiation	8.17 wt.%	≤26	[7]
					1.8	Anatase	Hydrothermal	0.05 wt.%	n.r.r.	[30]
Metolachlor	C ₁₅ H ₂₂ O ₂ NCl	22	3	0.14	0.15	Thin film (P25 doctor blade)	UV irradiation	0.001 M Ag ⁺	26	[31]
					0.1	Thin film (P25 doctor blade)	UV irradiation	0.1 M Ag ⁺	45	[31]
Orange II	C ₁₆ H ₁₁ N ₂ NaO ₄ S	10	1	0.10	1.5	Anatase (magnetic core)	Photodeposition	0.5 wt.%	n.r.r.	[32]
Methylene blue	C ₁₆ H ₁₈ ClN ₃ S	18	0	0	1.7	Thin film (dip coat)	Doped/calcined	2–4 mol%	2–10	[33]
					2.2 (fluor. light)	Thin film (rutile)	Neg. ion impl.	5 × 10 ¹⁶ ions/cm ²	1–2	[14]
					6.7 (UV cut)	Thin film (rutile)	Neg. ion impl.	5 × 10 ¹⁶ ions/cm ²	1–2	[14]
Brilliant X-3B	C ₁₉ H ₁₀ O ₇ N ₆ S ₂ Cl ₂ Na ₂	8	1	0.12	2.4	Degussa P25	n.r.r.	0.05 wt.%	n.r.r.	[34]
Basic blue 41	C ₁₉ H ₂₃ O ₂ N ₄ S	22	3	0.14	3	Thin film (dip coat)	Doped/calcined	10 mol%	n.r.r.	[35]
Astrazone orange G	C ₂₁ H ₂₂ N ₂ Cl	21	0	0	1.55 (pH 3.5)	Aldrich (anatase)	Depos./precip.	1 wt.%	n.r.r.	[13]
					4.5 (pH 7.0)	Aldrich (anatase)	Depos./precip.	1 wt.%	n.r.r.	[13]
Sirius gelb GC	C ₂₇ H ₁₀ O ₈ N ₆ SN ₂	17	6	0.35	2.5	Aldrich (anatase)	Depos./precip.	1 wt.%	n.r.r.	[36]

Included are ratio of (C–O + C=O):C–H bonds in organic, enhancement factor provided by Ag deposits, TiO₂ source and Ag deposition method, Ag loading on TiO₂ and Ag deposit size. All reactions occur in the liquid phase unless otherwise indicated. n.r.r.: no result reported.

^a British Drug House (BDH).

^b Yili Chemical Company (YCC).

due to preferential electron transfer from the TiO₂ surface to the silver deposits [11].

Studies by Vamathevan et al. [5] on phenol and salicylic acid indicated the presence of silver deposits did not alter the photocatalytic performance of TiO₂. They ascribed this effect for salicylic acid as due to its (and its intermediates) capability to act as deep hole traps and mediate efficient charge separation such that silver deposition did not significantly improve charge separation. For phenol, they postulated hole/electron recombination was promoted by an oxidation–reduction recombination cycle between the phenol oxidation intermediates, hydroquinone and benzoquinone. This suppressed any positive effects that silver deposits may have imposed.

The comparisons provided by Table 1 also illustrate the effects of silver deposits on photodegradation are not consistent for the same organic compound. Studies on 2-propanol by Sclafani and Herrmann [4] showed 0.5 wt.% silver to be beneficial for the photodegradation of 2-propanol when deposited on rutile but detrimental when deposited on anatase. Furthermore, in a separate paper, Sclafani et al. [10] showed different optimum silver loadings existed for different commercial TiO₂ sources and that these optimum loadings improved the removal of 2-propanol to different extents. Other aspects such as silver deposition method [12] and reactor configuration during photodegradation can influence the performance of the silver deposits. Table 1 also indicates attributes such as pH (Astrazone Orange G [13]) and light source (methylene blue [14]) can be influential.

As well as the effects imparted by characteristics of the silver-deposited TiO₂ and the photoreaction system on organic degradation, the molecular structure of the organic has to be considered. The presence and location of various functional groups (e.g. carboxylic and alcoholic), aromatic rings, multiple bonds and heteroatoms (e.g. N, Cl, S) within an organic define the characteristics of the organic and govern the mechanism, rate and enhancement/detriment imposed by silver deposits. Studies by Jiang et al. [15], Assabane et al. [16], Yu et al. [17] and Bouquet-Somrani et al. [18] have illustrated the effect minor changes in organic structure have on photooxidation by bare TiO₂ but no evidence of similar studies on Ag/TiO₂ has been found to date. This paper presents the early stages of work undertaken to investigate the effect of organic composition and structure on the photocatalytic results invoked by silver deposits on TiO₂. In particular, it considers organics containing only C, H and O atoms, as other heteroatoms may impart additional effects and are beyond the scope of this work. The study then investigates the degradation of selected organics in greater detail with the aim of identifying issues, which influence the photodegradation process.

2. Experimental

2.1. Chemicals

Ultra-pure water (Millipore, Mili-Q Plus) was used for all solutions. Stock solutions of organic compounds were prepared from analytical grade chemicals including sucrose (>99% pure,

Fisons Scientific Equipment), salicylic acid, phenol, methanol, formic acid, acetic acid, malonic acid, *iso*-butyric acid (>99% pure Aldrich), *n*-hexanol (>99% pure, Ajax Chemicals) and oxalic acid (>99% pure, Sigma–Aldrich). All stock solutions have the same concentration of 1 mg C/mL except salicylic acid whose concentration was 0.4 mg C/mL. The titanium dioxide source was Degussa P25 having a BET specific surface area of 55 ± 15 m²/g and an average crystallite size of 30 nm [3]. Silver was sourced from a 0.1 M stock solution of silver nitrate (AgNO₃ 99.9999 wt.% Aldrich Chemical). Diluted 0.1 M perchloric acid (70 wt.% analytical grade, Aldrich Chemical) was used for pH adjustment.

2.2. Ag/TiO₂ preparation

An annular photoreactor, as described elsewhere [37], which has an operational volume of 600 mL, was used to prepare Ag/TiO₂. A NEC 20 W blacklight blue lamp (emission range 300–400 nm with a peak emission at 355 nm), located concentric to the photoreactor, provided the source of UVA irradiation. A 500 mL TiO₂ suspension at a concentration of 1 g/L TiO₂ was first sonicated for 30 min in order to de-aggregate the TiO₂ particles. The solution was then transferred to the photoreactor, and circulated through the system by means of a peristaltic pump. With the lamp switched off, silver nitrate was added to the suspension to give an Ag:Ti atom ratio of 2%. Two millilitres of 83 mM methanol (equivalent to 2000 µg carbon (C)), which acted as a hole scavenger, was added and mixed with the TiO₂ suspension. After mixing for 10 min in the dark, the suspension was illuminated for 1 h. Particles of Ag/TiO₂ were recovered by centrifugation (10,000 rpm for 10 min) followed by washing with Milli-Q water. The centrifugation–washing step was repeated five times to ensure the removal of residual ions and organic precursors. The recovered particles were dried at 60 °C in an oven for 2 days, ground and stored in a desiccator.

2.3. Degradation experiments

The reactor setup (Fig. 1) for degradation experiments is similar to that described by Vamathevan et al. [3]. Photocatalytic oxidation was conducted in a twin spiral, slurry-type, batch photoreactor. Two borosilicate glass coils in series (2) were irradiated by dual blacklight lamps (NEC, 15 W, maximum emission at 350 nm, emission range 300–400 nm). The photocatalyst suspension was circulated using a peristaltic pump (5) and CO₂ detection was achieved by a gas–liquid separator (1), a liquid trap (6) coupled to a conductivity cell (3) and meter (4). CO₂ production is directly related to the extent of mineralisation of the target organic.

The pH of 50 mL of photocatalyst slurry at a concentration of 1 g/L was adjusted to 3.5 ± 0.5 and circulated through the photoreactor at a flow rate of 2 mL/s. The target organic compound (amount equivalent to 2000 µg C) was then injected and mixed under dark conditions for 10 min. The slurry was irradiated and the conductivity reading was recorded regularly until a stable conductivity value was attained. This marked the completion of mineralisation. Total organic carbon (TOC) analyses

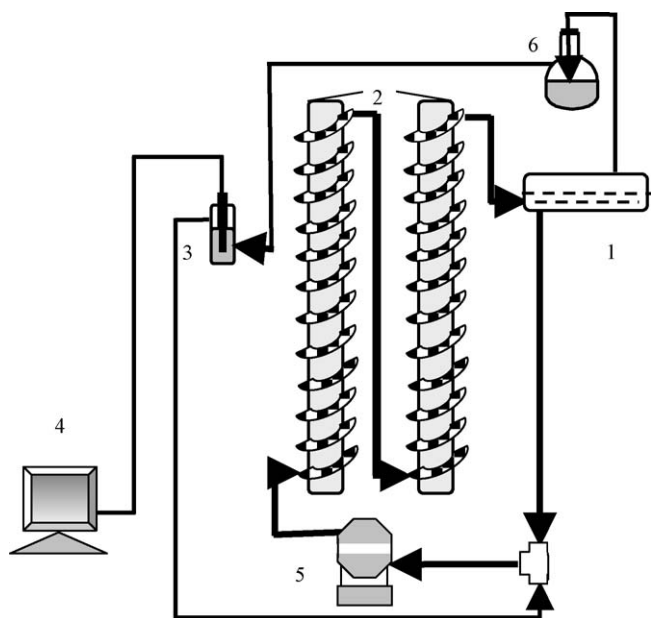


Fig. 1. Reactor arrangement. (1) Gas–liquid separator, (2) dual borosilicate glass coils, (3) conductivity cell, (4) conductivity meter, (5) peristaltic pump, and (6) liquid trap.

of the treated effluent were undertaken to confirm whether total mineralisation was achieved. Results are reported in terms of 15%, 50% and 90% mineralisation rates. These correspond to the average times taken to oxidise 15%, 50% or 90% of the organic carbon in the system, respectively. The 50% mineralisation results have been reported previously [38] but are included here for comparative purposes.

2.4. Adsorption studies

Five hundred millilitres of 0.1 g/L TiO₂ or 2 at.% Ag/TiO₂ suspension was ultrasonically mixed for 30 min before placement in an annular photocatalytic reactor. Oxalic acid, methanol, sucrose, or salicylic acid was then added to the suspension (amount equivalent to 20,000 μg C) and mixed for 15 min in the dark. The suspension was illuminated and samples were withdrawn regularly and their zeta potential measured to assess the

surface charge of the photocatalyst during degradation reactions. Organic addition led to a further decrease in pH to below 3.5, depending on the pK_a value of the organic. Given the proximity of this pH to the pH_{pzc} of TiO₂ (~5.5) shifts in zeta potential due to the pH drop were found to be negligible. The effect of UV-irradiation alone on the zeta potential of Degussa P25 has been shown by Lam et al. as negligible [39].

2.5. Characterisation techniques

The mass of silver deposited on the TiO₂ surface was quantified using inductively coupled plasma atomic emission spectroscopy (Varian Vista AX CCD Simultaneous). Ag/TiO₂ digestion was by hot concentrated nitric acid.

TOC analysis (TOC-V CSH Total Organic Carbon Analyzer-Shimadzu) was used to measure the carbon content remaining in solution following irradiation in the presence of either bare TiO₂ or Ag/TiO₂. Zeta potential measurements were carried out using a Brookhaven Zeta Plus for assessing the surface charge of the particles.

The morphology of silver deposits on the TiO₂ surface was determined by transmission electron microscopy (TEM) using a Philips CM 200 field emission gun microscope. Scanning transmission electron microscope-energy dispersive X-ray (STEM-EDX) analyses were used to identify particle composition.

3. Results and discussion

3.1. Photocatalyst characterisation

TEM micrographs (Fig. 2) of 2 at.% Ag/TiO₂ particles indicate a predominance of Ag deposits on the surface of TiO₂ with a diameter approximately 5 nm (Fig. 2(a)). Randomly located throughout the sample were a small number of larger Ag deposits, approximately 100 nm in diameter (Fig. 2(b)). STEM-EDX confirmed the large deposit in Fig. 2(b) to be silver.

Table 1 provides a summary of reported Ag deposit sizes on TiO₂ for various TiO₂ supports, deposition methods and silver loadings. The summary indicates deposit sizes are generally ≤10 nm in diameter when Ag loadings are ≤8 wt.%. Therefore,

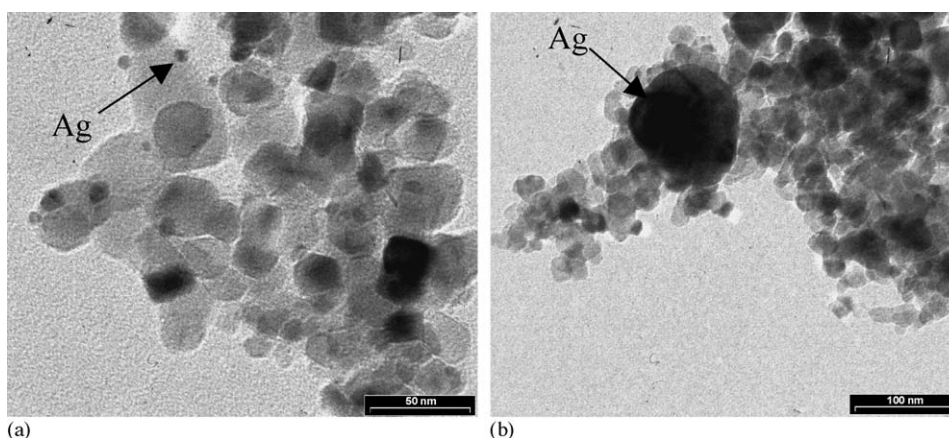


Fig. 2. TEM micrographs of 2 at.% Ag/TiO₂ after 60 min illumination.

while the presence of Ag deposits of 5 nm diameter are not unexpected here, the presence of large silver deposits ~ 100 nm diameter is. Ag deposits in the size range 100 nm and greater have been reported by Vamathevan et al. [3] and Herrmann et al. [40] but this was at silver loadings of 20 at.% and 38 wt.%, respectively. Su et al. [2] reported the presence of silver deposits as large as 90 nm for 3 wt.% Ag/TiO₂ prepared by photodeposition. They utilised a 200 W Hg arc lamp during deposition and also found that at shorter irradiation times (30 min) the Ag deposits possessed diameters <10 nm. The reasons for the larger isolated silver deposits occurring during preparation of our Ag/TiO₂ particles are unclear at this point in time.

3.2. Photocatalytic mineralisation under ambient conditions

The effects of silver deposited TiO₂ on the average mineralisation rate at 15%, 50% and 90% mineralisation of 14 organic compounds are shown in Fig. 3. For ease of comparison, the compounds have been classed into four groups: (1) the saccharide group including sucrose, glucose and fructose; (2) the carboxylic acid group including formic, acetic, *iso*-butyric, oxalic, malonic, maleic and citric acids; (3) the aromatic organics including salicylic acid and phenol; and (4) the alcoholic group including methanol and *n*-hexanol.

Fig. 3 indicates the silver deposits significantly improve the mineralisation rates for the saccharides and the majority of the carboxylic acids at the three average mineralisation rates considered. Alternately, silver deposits had a negligible or mildly detrimental effect on the mineralisation of aromatic and alcoholic compounds. These three values illustrate the effect of silver deposits over the complete mineralisation curve. They show in general the effects imparted by the silver deposits are consistent over the complete mineralisation process for each organic. The extent to which the silver modified the 15%, 50% and 90% mineralisation rates of each of these compounds is given in Table 2. The mineralisation rate effect values were determined by:

$$x\% \text{ mineral. rate effect} = \frac{\text{average mineralisation rate at } x\% \text{ carbon mineralised by Ag/TiO}_2}{\text{average mineralisation rate at } x\% \text{ carbon mineralised by bare TiO}_2}$$

Mineralisation of the saccharides and carboxylic acid groups appears to be predominantly enhanced by the silver deposits, whereas the aromatics and alcohols are not. This implies the molecular structure of the organic plays a role in defining the effects conveyed by the silver deposits to the photocatalytic process. The type and location of functional groups within the organic structure, chain branching and the presence of aromatic rings will govern bond strengths, radical and hole attack points and the degree to which the molecule adsorbs on the TiO₂ surface. This in turn will influence the mechanisms and reaction pathways favoured during the photodegradation process.

3.2.1. Mono-carboxylic acids

Fig. 3 indicates that, apart from *iso*-butyric acid, mineralisation of the mono-carboxylic acids considered (formic, acetic and *iso*-butyric acids) is enhanced in the presence of silver deposits. Of these, formic acid undergoes significant enhancement in the

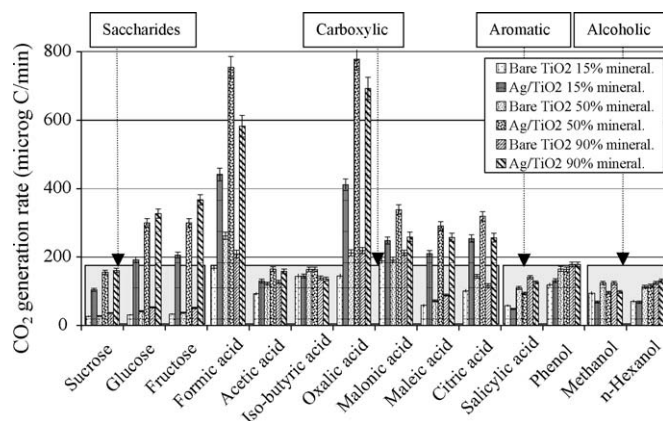
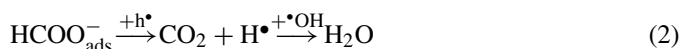


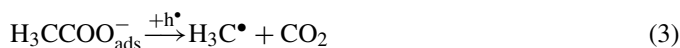
Fig. 3. Average mineralisation rates for the oxidation of 15%, 50% and 90% of the total carbon available for selected organic compounds by bare TiO₂ and 2 at.% Ag/TiO₂.

presence of silver, whereas acetic and *iso*-butyric acid undergo only minor or negligible enhancement, respectively. It therefore appears the presence of methyl groups within the molecule decreases the positive effects imparted by silver deposits.

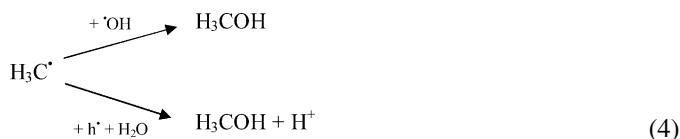
Simple mono-carboxylic acids are known to dissociatively adsorb on the surface of TiO₂ [41] via the two oxygen molecules of the carboxyl group in a bi-dentate configuration with the carbon chain perpendicular to the surface. Such an arrangement leaves the carboxyl group open to hole attack so an increase in hole availability should accelerate oxidation. Silver deposits increase hole availability, in turn providing the observed increase in mineralisation rates. This is especially the case for formic acid as, following dissociation (Eq. (1)), it requires only a single oxidation step for mineralisation (Eq. (2)):



In the case of acetic acid, following oxidation of the dissociated carboxylate group, a methyl radical remains (Eq. (3)):

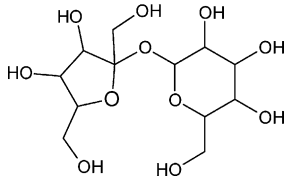
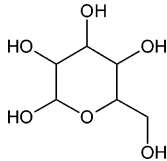
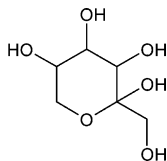
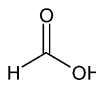
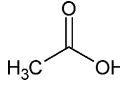
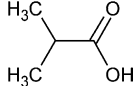
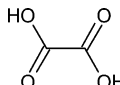
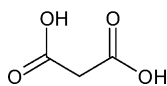
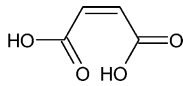
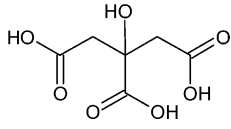
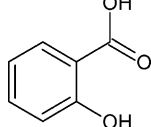
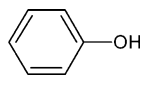
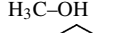



This methyl radical can then react with hydroxyl radicals or positive holes to give methanol (Eq. (4)):



Methanol photodegrades via a series of steps, forming formaldehyde and formic acid as intermediates in the process, to give CO₂ [42,43]. As is shown later, methanol does not extensively adsorb on TiO₂, so no substantial improvements should be imparted by the silver deposits during photooxidation of the methanol to give

Table 2
Molecular structure of organic compounds, corresponding (C–O/C=O):C–H bond ratios and 15%, 50% and 90% mineralisation rate changes provided by Ag/TiO₂ relative to bare TiO₂

Organic	Molecular structure	Bond ratio (C–O, C=O):C–H	Mineralisation rate effect		
			15%	50%	90%
Sucrose C ₁₂ H ₂₂ O ₁₁		1.00	3.9	5.7	4.4
Glucose C ₆ H ₁₂ O ₆		1.00	6.1	7.2	6.2
Fructose C ₆ H ₁₂ O ₆		1.00	6.1	8.0	7.1
Formic acid CH ₂ O ₂		2.00	2.6	2.9	2.8
Acetic acid C ₂ H ₄ O ₂		0.67	1.4	1.3	1.2
<i>iso</i> -Butyric acid C ₄ H ₈ O ₂		0.29	1.0	1.0	1.0
Oxalic acid C ₂ H ₂ O ₄		4.00	2.8	3.7	3.2
Malonic acid C ₃ H ₄ O ₄		2.00	1.3	1.8	1.2
Maleic acid C ₄ H ₄ O ₄		2.00	3.6	4.0	2.9
Citric acid C ₆ H ₈ O ₇		1.75	2.5	2.2	2.2
Salicylic acid C ₇ H ₆ O ₃		0.75	0.8	0.9	0.9
Phenol C ₆ H ₆ O		0.20	1.1	1.0	1.0
Methanol CH ₄ O		0.33	0.7	0.8	0.8
<i>n</i> -Hexanol C ₆ H ₁₄ O		0.08	1.0	1.0	1.1

Mineralisation rate effect corresponds to the mineralisation rate of Ag/TiO₂ over the mineralisation rate of bare TiO₂ at a defined percentage of carbon oxidised. Values <1 indicate a detrimental effect of Ag deposits.

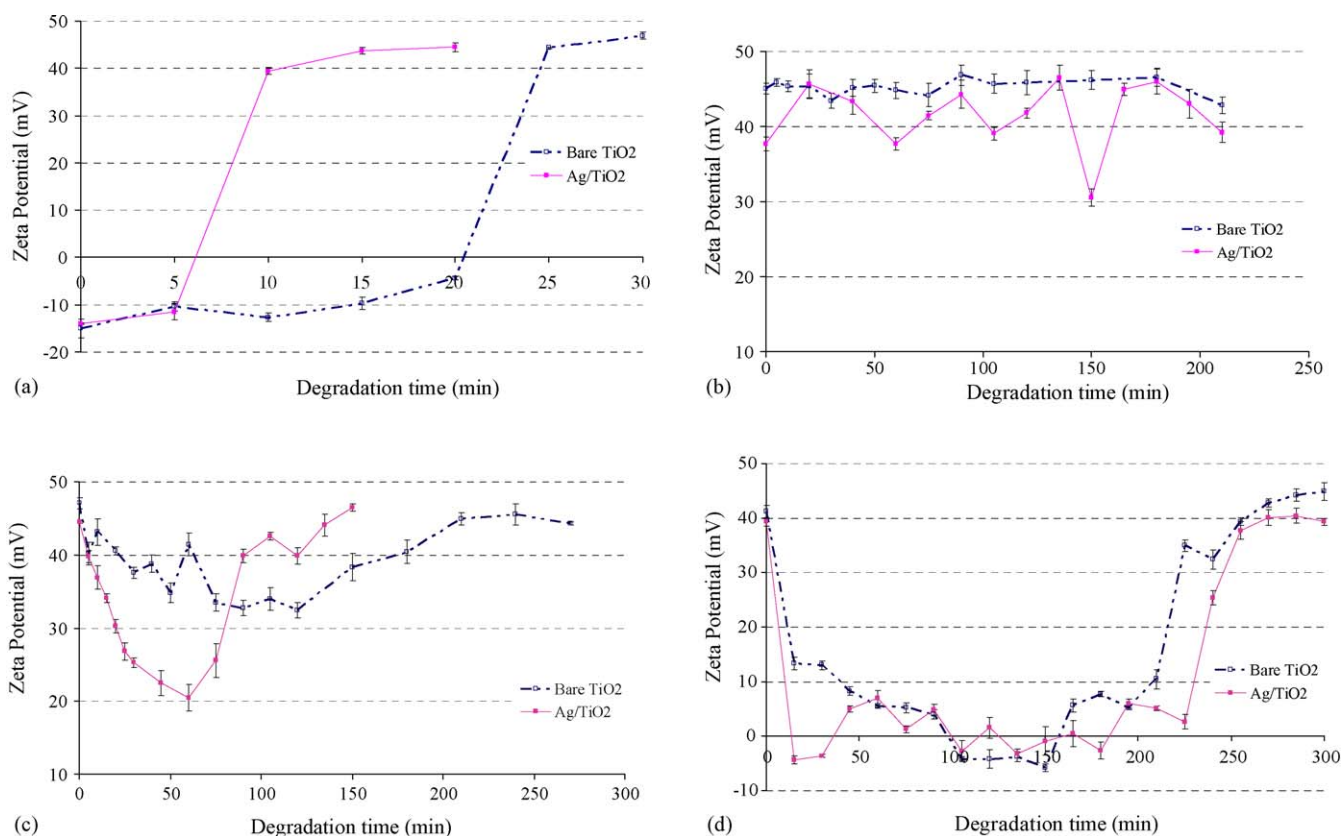
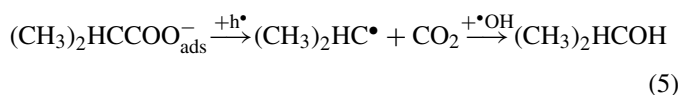


Fig. 4. Zeta potential of bare TiO₂ and 2 at.% Ag/TiO₂ for (a) oxalic acid; (b) methanol; (c) sucrose; (d) salicylic acid. Photocatalyst loading = 0.1 g/L. Initial organic concentration = 40 ppm carbon.

formaldehyde. It is suspected this oxidation step limits any significant positive effects displayed by the silver deposits for acetic acid.

Similarly for *iso*-butyric acid, following oxidation of the dissociated carboxylate group, isopropanol is produced (Eq. (5)):



Isopropanol must progress through a series of intermediate reaction steps in order to mineralise the remaining carbons, a number of which may not occur on the TiO₂ surface, leading to no observable positive effects of the silver deposits.

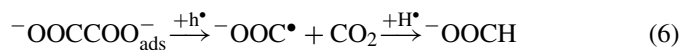
3.2.2. Di- and poly-carboxylic acids

Fig. 3 indicates, of the dicarboxylic acids considered, oxalic acid experiences the greatest overall average rate of mineralisation in the presence of silver deposits. In terms of the relative enhancement provided by the silver, oxalic acid and maleic acid are enhanced to similar extents, with malonic acid being significantly lower (Table 2).

The adsorption of oxalic acid on the surface of TiO₂ has been investigated by others [44,45] with a variety of adsorption modes proposed. These studies suggest oxalic acid adsorbs dissociatively, with the most stable configuration being the two dissociated hydroxyl groups of the oxalate bonded to a single Ti atom. Fig. 4(a) confirms oxalic acid adsorption where the initial

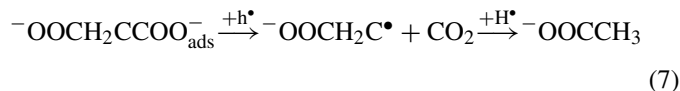
adsorption of oxalic acid on TiO₂ is illustrated by the change in zeta potential of TiO₂ in the presence of oxalic acid. Here it can be seen the oxalic acid alters the surface charge of the bare TiO₂ from +45 to -15 mV. The effect is similar for Ag/TiO₂.

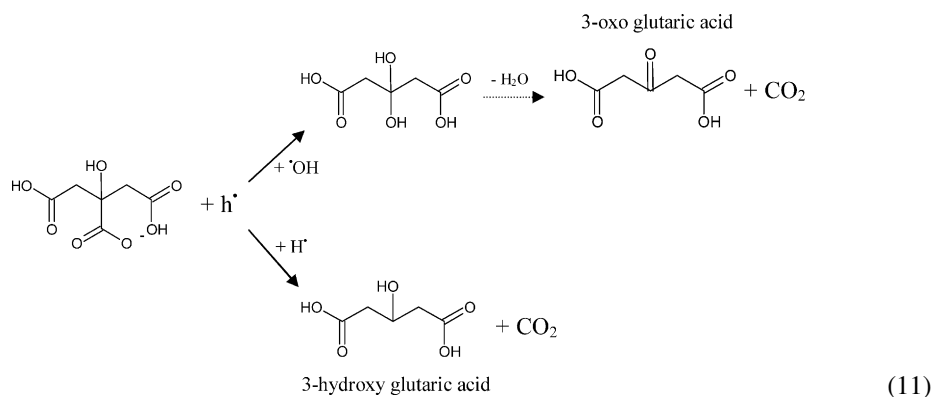
The dissociatively adsorbed oxalic acid can then be attacked by photogenerated holes to give formate ions (Eq. (6)):



As discussed previously, formate ions are readily adsorbed on TiO₂ and rapidly mineralised, particularly in the presence of silver deposits. The acceleration in mineralisation offered by the silver deposits is seen in Fig. 4(a) whereby the shift in zeta potential to its original value, following irradiation, is much quicker than for bare TiO₂. This shift corresponds to the mineralisation/removal of organics on/from the TiO₂ surface, as confirmed by subsequent TOC measurements. Szabó-Bárdos et al. [19] have reported enhancement in the photodegradation of oxalic acid by a factor of five in the presence of silver deposits (Table 1).

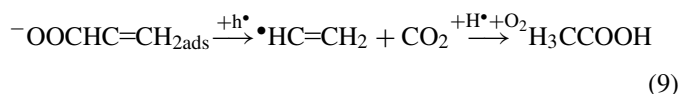
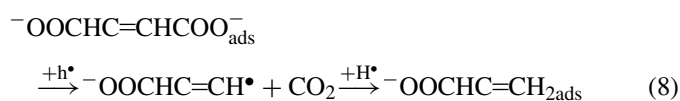
The enhancement effect provided by silver deposits for malonic acid is much less pronounced than oxalic acid. Malonic acid contains an additional carbon in its chain which, following photooxidation of one of the carboxyl groups, can give acetic acid (Eq. (7)). The mode of adsorption of malonic acid is not clear here and has been assumed similar to that for oxalic acid:





As discussed previously, acetic acid is slower to mineralise than formic acid, which may contribute to the different rates observed for malonic and oxalic acids.

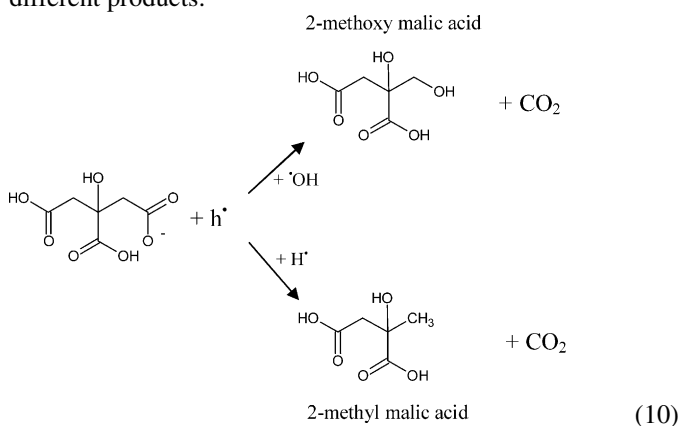
The presence of silver deposits enhances the mineralisation of maleic acid by a factor of up to four (Table 2). This increase is comparable with oxalic acid, however, Fig. 3 shows the overall mineralisation rates of maleic acid are much lower and more comparable with malonic acid for the silver deposited samples. Franch et al. [46] describes the most likely maleic acid degradation pathway at $\text{pH} < \text{pH}_{\text{pzc}}$ to be via acrylic acid (Eq. (8))/acetic acid (Eq. (9)) formation:



The presence of acetic acid in the degradation mechanism may again be the limiting factor in the enhancement provided by the silver deposits.

Herrmann et al. [6] found maleic acid, a hydroxylated dicarboxylic acid, experienced a four times increase in degradation rate in the presence of silver deposits (Table 1).

Citric acid possesses three carboxylic acid groups, one at each end of the carbon chain and one attached to the central carbon of this chain. It is unclear as to the exact mode of adsorption and photodegradation of this molecule as attachment to the TiO_2 surface by either of the end carboxyl groups (Eq. (10)) or the central group (Eq. (11)) and subsequent hole attack will give different products:



Currently these initial steps are only postulated and require further assessment to confirm their likelihood.

3.2.3. Alcohols

Fig. 3 and Table 2 indicate the presence of silver deposits on TiO_2 has a detrimental effect on the mineralisation of methanol and a negligible effect on the mineralisation of *n*-hexanol. Methanol adsorption on TiO_2 has been reported by Henderson et al. [47,48] to occur predominantly at sub-ambient temperatures. They reported the majority of molecules adsorbed intact (i.e. no dissociation) and left the surface at around 295 K. Zeta potential measurements (Fig. 4(b)) support this finding showing minimal evidence of methanol adsorption on either bare or silver-deposited TiO_2 at room temperature in this system. The fact methanol does not adsorb extensively on the TiO_2 surface at room temperature assists in explaining the negative impact of the silver deposits. The increased generation of positive holes is of minimal benefit to the methanol as it remains predominantly in solution. Here it is attacked by hydroxyl radicals to give formaldehyde (Eq. (12)):



Fig. 4(b) indicates during the photodegradation process neither methanol nor any of the generated intermediates are adsorbed on the surface of either photocatalyst. The decrease in mineralisation rate may be due to factors such as site blockage by the silver deposits as discussed previously.

Literature reports on the effect of silver deposits on the degradation of alcohols have indicated varying effects depending on the conditions used. Mildly positive effects of silver were reported by Sclafani and Herrmann [4] and Sclafani et al. [10] for the removal of isopropanol, apart from one instance where anatase was the support, whereas Chapuis et al. [21] found silver to have a detrimental effect on the gas phase removal of *n*-butanol.

3.2.4. Saccharides

Sucrose adsorbs sparingly on the surface of TiO_2 [5]. This is portrayed in Fig. 4(c) where the zeta potential of TiO_2 in a sucrose solution is the same as that without sucrose. Therefore, it would be expected the presence of silver deposits would not improve the mineralisation rate of the compound. As shown by Fig. 3 and Table 2, this is not the case with silver deposits

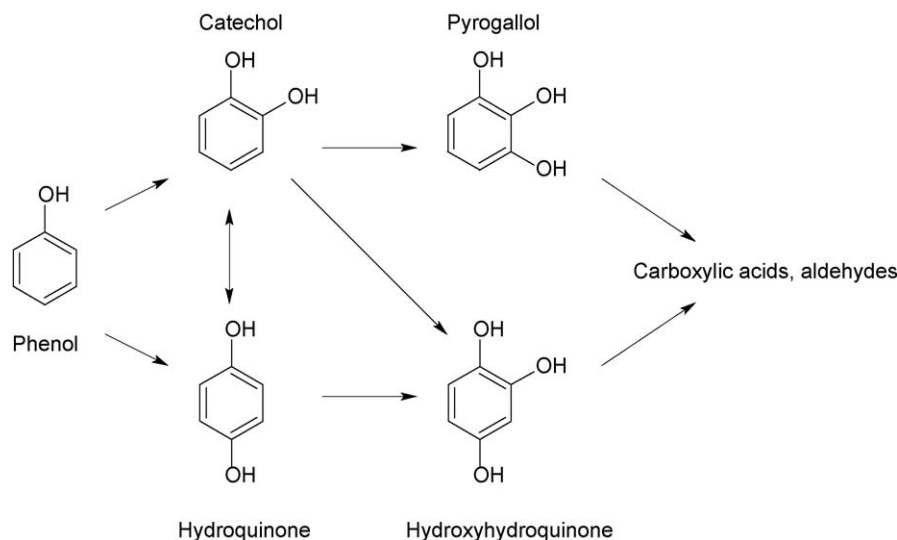


Fig. 5. Schematic of degradation steps during photooxidation of phenol. Source: Nagaveni et al. [52].

significantly enhancing the mineralisation of all saccharides considered. The reasons for this irregularity may be explained by the intermediates generated during the degradation process. Búriová et al. [49] determined intermediate products from the oxidation of glucose with Fenton's reagent to comprise of highly hydroxylated carboxylic acids such as arabonic acid ($23 \pm 2.1\%$), araburonic acid ($2.1 \pm 0.4\%$), gluconic acid ($12.1 \pm 2.3\%$) and glucuronic acid ($5.5 \pm 0.5\%$). The increase in mineralisation rate is thought to be due to the accelerated mineralisation of intermediates such as these by the silver deposits. Furthermore, Fig. 4(c) shows a decrease in the zeta potential of the TiO_2 and Ag/TiO_2 particles, indicative of the adsorption of intermediates on their surface. The lesser 'maximum' zeta potential value obtained for the bare TiO_2 is likely due to fewer intermediates being adsorbed on the surface. This may be caused by limits to the amount of intermediates available at any one time due to their lower rate of generation/degradation by the bare TiO_2 . TOC results confirmed complete mineralisation of sucrose occurred.

3.2.5. Aromatics

The extent of adsorption of phenol on TiO_2 has been reported in the literature to vary as a function of the titania source. Agrios and Pichat [50] reported no detectable adsorption of phenol ($150 \mu\text{mol/L}$ phenol with 20 g/L TiO_2) on a series of commercial Millennium Chemicals samples, following 18 h stirring. Medina-Valtierra et al. [51] reported phenol adsorption of $2 \text{ mg phenol/g catalyst}$ ($2 \text{ g/L catalyst loading}$) on Degussa P25 with equilibrium reached within 2 h while Nagaveni et al. [52] reported 10% adsorption of a 0.1 mM phenol solution mixed for 30 h with $0.1 \text{ g Degussa P25}$ (in 100 mL). Nagaveni et al. also reported that, within the first 2–3 h, phenol adsorption was not appreciable. On the basis of these values it is assumed in our system phenol remains largely in solution. This being the case, it is expected phenol will be predominantly degraded by hydroxyl radical attack. This idea is supported by Ilisz and Dombi [53] who suggested that, based on their results, in the presence of dissolved oxygen phenol decomposition proceeds mainly via

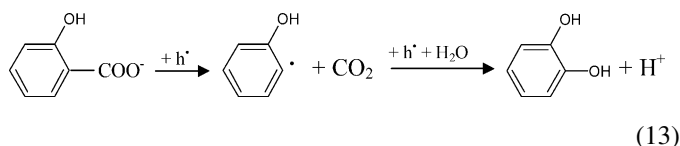
hydroxyl radical attack. Therefore, silver deposits should provide little improvement to the mineralisation of this compound. Fig. 3 and Table 2 show silver deposits have a negligible effect of phenol, supporting this reasoning.

In terms of the photodegradation mechanism of phenol it is well known that the pathway involves hydroxylation of the aromatic ring followed by eventual ring cleavage to form aldehydes and carboxylic acids. This is shown schematically in Fig. 5, sourced from Nagaveni et al. [52]. The formation of carboxylic acids as intermediates suggests the potential for acceleration of the mineralisation rate of phenol in the same fashion to that proposed for the saccharides and it is likely the formed carboxylic acids will experience an increased rate of degradation. However, if they have limited access to the TiO_2 surface or their degradation is not the original rate limiting step in the process then increasing their degradation rate will have an insignificant effect on the overall mineralisation rate. This latter possibility implies hydroxylation of the aromatic ring and/or ring cleavage may be the rate-limiting step during the degradation process. Araña et al. [54], when studying TiO_2 and Cu-TiO_2 for the photocatalytic oxidation of hydroxybenzenes, also tentatively suggested the early reaction stages seemed to govern the process rate.

Other literature reports [12,22,23] have predominantly found the presence of silver deposits to enhance phenol removal by up to 4.5 times. In these studies anatase was used as the TiO_2 support and they each considered the removal of phenol, not complete mineralisation. The presence of silver deposits may increase the hydroxylation of phenol during the initial steps of degradation but not contribute to the degradation of some of the generated intermediates. This may account for the difference in findings. Studies by Vamathevan et al. [5] on a similar system found silver provided negligible enhancement for the mineralisation of phenol postulated as due to charge recombination mediated by intermediate species.

The adsorption of salicylic acid on TiO_2 has been investigated by a number of workers [45,55]. They suggest salicylic acid can adsorb dissociatively either through its two hydroxyl groups on

a single titanium atom or via its carboxyl group to two adjacent Ti atoms. Of these, Weisz et al. [45] report the former to be the more stable although Kratochvilová et al. [55] report the later to be more favourable at higher salicylic loadings. Given the high organic concentrations used in this system the second adsorption mode is likely to be favoured. If this is the case, attack of the (dissociated) carboxyl group by positive holes will leave a hydroxide group in its place to give catechol (Eq (13)):



However, as seen in Fig. 4(d), the decrease in zeta potential prior to irradiation by the bare TiO₂ and Ag/TiO₂ in the presence of salicylic acid is small (~5 mV) compared to when no salicylic acid is present, indicating only limited adsorption occurs. This implies that, similar to phenol, the bulk of the salicylic acid remains in solution and will predominantly be degraded through hydroxyl radical attack.

The decrease in zeta potential upon illumination, shown in Fig. 4(d), indicates intermediate species from the degradation of salicylic acid are adsorbed on the surface of both TiO₂ and Ag/TiO₂. Moreover, there is little difference in the two zeta potential profiles, indicating the additional holes generated by the silver deposits do not facilitate increased degradation of these adsorbed intermediates. A similar zeta potential profile for the photodegradation of phenol by bare TiO₂ has been reported by Nagasaki et al. [56]. They explained the negative shift in zeta potential as due to the adsorption of catechol, pyrogallol and carboxylates produced during phenol degradation. Scheck and Frimmel [57] comprehensively investigated the degradation products from the oxidation of phenol and salicylic acid by a UV/H₂O₂/O₂ system. They showed, with the exception of the formation of 2,3-dihydroxybenzoic acid for salicylic acid, the intermediates formed from these two compounds were similar and included catechol, hydroquinone and muconic acid.

The findings for phenol and salicylic acid suggest photogenerated holes are unsuitable for degrading intermediates generated during the initial stages of photodegradation. Moreover, these intermediates appear to restrict availability of the TiO₂ sites necessary for carboxylic acid adsorption, as there is no observed enhancement of mineralisation rates in the latter stages of the process, the time when carboxylic acids are expected to be present in the system. Hydroxylated aromatics such as catechol and hydroquinone have been reported to adsorb on the surface of TiO₂ [58] with Heyd and Au [59] indicating catechol is strongly chemisorbed. In a similar vein, other aromatics such as benzene and toluene have been reported as difficult to degrade in dry gas phase applications, to the point of deactivating the TiO₂ [60,61]. In gas phase applications the predominant mode of degradation is expected to be by hole oxidation. This deactivation by aromatics in the gas phase lends support to the idea that photogenerated holes are not capable of assisting in the photodegradation of these early intermediates and therefore the effects imparted by silver deposits are minimal.

3.3. C–O/C=O:C–H bond ratio

The results have shown structural characteristics and the presence and type of functional groups on an organic molecule can influence the role of silver deposits in altering the performance of TiO₂. Generally, it appears carboxylic acid groups and molecules containing a large quota of hydroxyl groups (which form carboxylate groups during oxidation) profit from the presence of silver deposits, whereas alcohols and aromatics, which contain a proportionately high number of C–H bonds, are negligibly or negatively affected. Moreover, increasing the number of –CH₂– and –CH₃ groups in the organic suppresses the positive effects of silver deposits. These observations suggest a tentative screening method may be available to predict whether an organic may benefit from the presence of silver deposits during photodegradation. Comparing the ratio of the total C–O and C=O bonds to the total C–H bonds present in an organic with the effect of silver deposits on the mineralisation rate (Table 2) shows that for organics where the ratio is greater than or equal to one, enhancement is generally observed.

Further studies are being undertaken to confirm this but an assessment of the literature to support whether this observation holds is given in Table 1. The table has been divided into two classes of organics, those compounds containing C, H and O bonds only and those containing heteroatoms as well. Table 1 shows mixed results when comparing the bond ratio with the degree of enhancement provided by silver deposits. In the instance of organics containing only C, H and O bonds, cases where the bond ratio is greater than or equal to one provide substantial enhancement. In cases where the bond ratios are less than one silver deposits are detrimental for some organics and beneficial for others. This can be attributed to different TiO₂ sources, silver loadings, reactor systems etc., as discussed previously. Table 1 also suggests the presence of heteroatoms such as N, S and Cl within the organic may contribute to the beneficial effects imposed by silver deposits. A number of cases exist in Table 1 where, in organics containing various heteroatoms, no C–O or C=O bonds are present yet enhancement by silver deposits is evident. Further consideration is beyond the scope of this paper and constitutes future work.

4. Conclusions

The presence of silver deposits on TiO₂ was found to influence the mineralisation rate of a variety of organics in either a positive, mildly negative or negligible manner. Silver deposits facilitate charge separation, improving hole availability and when accessed by an organic compound may impart beneficial effects. Of the four groups of organics considered:

- i. Mono-, di- and poly-carboxylic acids predominantly experienced positive effects due to their ability to adsorb on the surface of TiO₂ and their susceptibility to hole attack. Increasing chain length or the presence of methyl groups generally decreased the enhancement provided by silver.
- ii. Alcohols experienced negligible or mildly negative effects due to silver deposition. As they undergo limited adsorption

on TiO₂ at room temperature they do not benefit from the greater hole availability invoked by the silver. The negative effects may be due to factors such as light shadowing by the deposits.

- iii. The saccharides all experienced significant increases in mineralisation rates for the Ag/TiO₂ particles. Saccharides are limited in their adsorption on TiO₂ however, the generated intermediates comprise highly hydroxylated carboxylic acids, which adsorb on TiO₂ and are readily attacked by holes.
- iv. The aromatics considered experienced negligible or mildly detrimental mineralisation rate effects in the presence of silver deposits. It is thought intermediates generated during the initial stages of degradation adsorb on the TiO₂ surface but are resistant to degradation by hole attack or may facilitate electron/hole recombination. Carboxylic acids generated in the latter stages of degradation do not benefit from silver deposition due to either limited access to the TiO₂ surface or the charge recombination effect. In other words, degradation of the carboxylic acids is not the rate-limiting step.

Comparison of the ratio of total C–O and C=O bonds to C–H bonds with enhancement provided by the silver deposits indicated for a bond ratio ≥ 1 enhancement is generally observed. This result is only tentative given the limited number of compounds considered at this time. Further studies on a greater number and variety of compounds are required to support this finding.

Acknowledgements

The authors would like to thank the Vietnam Ministry of Training and Education for financial assistance provided through the D322 Project. Financial support by the ARC (Australian Research Council) Centre for Functional Nanomaterials is greatly acknowledged. Thanks to Mrs. Katie Levick for her assistance with electron microscopy analysis.

References

- [1] M.I. Litter, *Appl. Catal. B: Environ.* 23 (1999) 89.
- [2] C. Su, C.-H. Liao, J.-D. Wang, C.-M. Chiu, B.-J. Chen, *Catal. Today* 97 (2004) 71.
- [3] V. Vamathevan, R. Amal, D. Beydoun, G. Low, S. McEvoy, *J. Photochem. Photobiol. A: Chem.* 148 (2002) 233.
- [4] A. Scalfani, J.-M. Herrmann, *J. Photochem. Photobiol. A: Chem.* 113 (1998) 181.
- [5] V. Vamathevan, R. Amal, D. Beydoun, G. Low, S. McEvoy, *Chem. Eng. J.* 98 (2004) 127.
- [6] J.-M. Herrmann, H. Tahiri, Y. Ait-Ichou, G. Lassaletta, A.R. González-Elipe, A. Fernández, *Appl. Catal. B: Environ.* 13 (1997) 219.
- [7] I.M. Arabatzis, T. Stergiopoulos, M.C. Bernard, D. Labou, S.G. Neophytides, P. Falaras, *Appl. Catal. B: Environ.* 42 (2003) 187.
- [8] M.R. Dhananjeyan, R. Annapoorani, R. Renganathan, *J. Photochem. Photobiol. A: Chem.* 109 (1997) 147.
- [9] D.H. Kim, M.A. Anderson, *J. Photochem. Photobiol. A: Chem.* 94 (1996) 221.
- [10] A. Scalfani, M.-N. Mozzanega, P. Pichat, *J. Photochem. Photobiol. A: Chem.* 59 (1991) 181.
- [11] H. Tahiri, Y.A. Ichou, J.-M. Herrmann, *J. Photochem. Photobiol. A: Chem.* 114 (1998) 219.
- [12] A. Dobosz, A. Sobczyński, *Water Res.* 37 (2003) 1489.
- [13] M. Sökmen, A. Özkan, *J. Photochem. Photobiol. A: Chem.* 147 (2002) 77.
- [14] H. Tsuji, H. Sugahara, Y. Gotoh, J. Ishikawa, *Nucl. Instrum. Methods: Phys. Res. B* 206 (2003) 249.
- [15] D. Jiang, H. Zhao, S. Zhang, R. John, *J. Catal.* 223 (2004) 212.
- [16] A. Assabane, Y.A. Ichou, H. Tahiri, C. Guillard, J.-M. Herrmann, *Appl. Catal. B: Environ.* 24 (2000) 71.
- [17] K.-P. Yu, G.W.M. Lee, W.M. Huang, C. Wu, S. Yang, *Atmos. Environ.* 40 (2006) 375.
- [18] C. Bouquet-Somrani, A. Finiels, P. Gaffin, J.-L. Olivé, *Appl. Catal. B: Environ.* 8 (1996) 101.
- [19] E. Szabó-Bárdos, H. Czili, A. Horváth, *J. Photochem. Photobiol. A: Chem.* 154 (2003) 195.
- [20] L. Zhang, J.C. Yu, H.Y. Yip, Q. Li, K.W. Kwong, A.-W. Xu, P.K. Wong, *Langmuir* 19 (2003) 10372.
- [21] Y. Chapuis, D. Klvana, C. Guy, J. Kirchnerova, *JAWMA* (2002) 845.
- [22] I. Illisz, Z. László, A. Dombi, *Appl. Catal. A: Gen.* 180 (1999) 25.
- [23] S.X. Liu, Z.P. Qu, X.W. Han, C.L. Sun, *Catal. Today* 93–95 (2004) 877.
- [24] M.M. Kondo, W.F. Jardim, *Water Res.* 25 (1991) 823.
- [25] S. Kato, Y. Hirano, M. Iwata, T. Sano, K. Takeuchi, S. Matsuzawa, *Appl. Catal. B: Environ.* 57 (2004) 109.
- [26] J.C. Crittenden, J. Liu, D.W. Hand, D.L. Perram, *Water Res.* 31 (1997) 429.
- [27] D. Shchukin, E. Ustinovich, D. Sviridov, P. Pichat, *Photochem. Photobiol. Sci.* 3 (2004) 142.
- [28] A. Kumar, N. Mathur, *Appl. Catal. A: Gen.* 275 (2004) 189.
- [29] X. You, F. Chen, J. Zhang, M. Anpo, *Catal. Lett.* 102 (2005) 247.
- [30] Y. Liu, C. Lui, Q. Rong, Z. Zhang, *Appl. Surf. Sci.* 220 (2003) 7.
- [31] V.A. Sakkas, I.M. Arabatzis, I.K. Konstantinou, A.D. Dimou, T.A. Albanis, P. Falaras, *Appl. Catal. A: Environ.* 49 (2004) 195.
- [32] M.-W. Xu, S.-J. Bao, X.-G. Zhang, *Mater. Lett.* 59 (2005) 2194.
- [33] C. He, Y. Yu, X. Hu, A. Larbot, *Appl. Surf. Sci.* 200 (2002) 239.
- [34] X.-H. Qi, Z.-H. Wang, Y.-Y. Zhuang, Y. Yu, J. Li, *J. Hazard. Mater. B* 118 (2005) 219.
- [35] E. Stathatos, T. Petrova, P. Lianos, *Langmuir* 17 (2001) 5025.
- [36] A. Özkan, M.H. Özkan, R. Gürkan, M. Akcay, M. Sokmen, *J. Photochem. Photobiol. A: Chem.* 163 (2004) 29.
- [37] S.W. Lam, K. Chiang, T.M. Lim, R. Amal, G. Low, *Appl. Catal. B: Environ.* 55 (2005) 123.
- [38] H. Tran, K. Chiang, J. Scott, R. Amal, *Photochem. Photobiol. Sci.* 4 (2005) 565.
- [39] S.W. Lam, K. Chiang, T.M. Lim, R. Amal, G.K.-C. Low, *Proceedings of 2005 CHEMECA, Hilton Hotel, Brisbane, Queensland, Australia, September 25–28, 2005.*
- [40] J.M. Herrmann, J. Disdier, P. Pichat, *J. Catal.* 113 (1988) 72.
- [41] U. Diebold, *Surf. Sci. Rep.* 48 (2003) 53.
- [42] M.J. Bakes, A.C. Lukaski, D.S. Muggli, *Appl. Catal. B: Environ.* 61 (2005) 23.
- [43] J. Araña, J.M. Doña Rodríguez, O. González Díaz, J.A. Herrera Melián, J. Pérez Peña, *Appl. Surf. Sci.*, in press.
- [44] A. Fahmi, C. Minot, P. Fourré, P. Nortier, *Surf. Sci.* 343 (1995) 261.
- [45] A.D. Weisz, R.L. García Rodenas, P.L. Morando, A.E. Regazzoni, M.A. Blesa, *Catal. Today* 76 (2002) 103.
- [46] M.I. Franch, J.A. Ayllón, J. Peral, X. Domènech, *Catal. Today* 76 (2002) 221.
- [47] M.A. Henderson, S. Otero-Tapia, M.E. Castro, *Surf. Sci.* 412 (1998) 252.
- [48] M.A. Henderson, S. Otero-Tapia, M.E. Castro, *Faraday Discuss. Chem. Soc.* 114 (1999) 313.
- [49] E. Búriová, M. Medová, F. Macásek, P. Brúder, *J. Chromatogr. A* 1034 (2004) 133.
- [50] A.G. Agrios, P. Pichat, *J. Photochem. Photobiol. A: Chem.* 180 (2006) 130–135.
- [51] J. Medina-Valtierra, E. Moctezuma, M. Sánchez-Cárdenas, C. Frausto-Reyes, *J. Photochem. Photobiol. A: Chem.* 174 (2005) 246.
- [52] K. Nagaveni, G. Sivalingam, M.S. Hegde, G. Madras, *Environ. Sci. Technol.* 38 (2004) 1600.
- [53] I. Illisz, A. Dombi, *Appl. Catal. A: Gen.* 180 (1999) 35.

- [54] J. Araña, C. Fernández Rodríguez, O. González Díaz, J.A. Herrera Melián, J. Pérez Peña, *Catal. Today* 101 (2005) 261.
- [55] K. Kratochvilová, I. Hoskocová, J. Jirkovský, J. Klíma, J. Ludvík, *Electrochim. Acta* 40 (1995) 2603.
- [56] A. Nagasaki, H. Sakai, M. Shimazaki, T. Kakihara, T. Kono, N. Momozawa, M. Abe, *Shikizai Kyokaishi* 72 (1999) 665.
- [57] C.K. Scheck, F.H. Frimmel, *Water Res.* 29 (1995) 2346.
- [58] A. Sobczyński, L. Duczmal, W. Zmudziński, *J. Mol. Catal. A: Chem.* 213 (2004) 225.
- [59] D.V. Heyd, B. Au, *J. Photochem. Photobiol. A: Chem.* 174 (2005) 62.
- [60] O. d'Hennezel, P. Pichat, D.F. Ollis, *J. Photochem. Photobiol. A: Chem.* 118 (1998) 197.
- [61] S.B. Kim, H.T. Hwang, S.C. Hong, *Chemosphere* 48 (2002) 437.